JOURNAL OF SOLID STATE CHEMISTRY 110, 6–14 (1994)

Variable Electrical Properties in Composites: Application to Vanadium Dioxide Pigments in a Polyethylene Host

Carole Alfred-Duplan,*,† Jean Musso,* Jean-Raymond Gavarri,*,†,[1] and Claude Cesari*

*Laboratoire des Matériaux Multiphasés et Interfaces, Université de Toulon et du Var, BP 132, 83 9578 La Garde Cédex, France; and †Laboratoire MATOP (U.A. au CNRS), Université Aix-Marseille III, Centre St-Jérôme, 13 397 Marseille Cédex, France

Received December 28, 1992; in revised form May 10, 1993; accepted May 13, 1993

Composite pellets were prepared from low-density polyethylene (LDPE) and vanadium dioxide powders. The VO_2 pigments are used for their insulating-to-metallic transition at 341 K in order to obtain electrically variable composite materials. The volume fractions of VO_2 powders vary from $\phi = 0$ to $\phi = 0.55$. The composite samples are characterized by X-ray diffraction and scanning electron microscopy. Complex impedance analysis in the frequency range 10^{-1} to 10^6 Hz is carried out at room temperature and at $T = 363$ K, to observe the insulator–metal transition of VO_2 pigments dispersed in the polymer host. The variation of the complex impedance modulus $|Z|$ with frequency and with VO_2 volume fraction (ϕ) is discussed. A specific (R, C) impedance model permits interpretation of the experimental results in terms of percolation; the observed variations can be accounted for.

I. INTRODUCTION

The general aim of this study was to test composite materials composed of organic polymer and oxide pigments presenting a phase transition. The insulator-to-metal transition (1 to 6) at $T_c = 341$ K vanadium dioxide VO_2 can be used to realize an electrically switching composite material having interesting elastic and mechanical properties. In previous works (7–12), the various optical, structural, and thermodynamic switching properties of substituted samples $V_{1-x}W_xO_2$ ($x = 0$ to 0.02) were investigated. Here we deal with the variation of electrical properties of a polyethylenal VO_2 composite material.

II. EXPERIMENTAL STUDY

II.1. Samples

The preparation of cylindrical pellets ($D = 20$ mm, $h = 3$–7 mm) was carried out in order to perform direct analyses of the final material.

—1. A powdered VO_2 ceramic (Aldrich) was used: the granularity is such that the maximum grain size is 38 μm (density = 4.68).

—2. The polymer host is obtained from powdered, low-density polyethylene (Aldrich; notation LDPE) with density 0.91.

—3. The initial mixtures are obtained for various weight fractions; see Table 1.

—4. The pellets are obtained by heating at 140°C (413 K) under hydrostatic pressure during a fixed t_1 duration in air; the samples are then cooled at controlled cooling rates.

Each sample, denoted P_i ($i = 1$ to 12), is characterized by its effective volumic weight μ_{Obs} (Table 1) which includes three different volume fractions ϕ associated with VO_2 pigments (ϕ_{VO_2}), polyethylene host (both amorphous and crystallized parts; ϕ_{POL}), and cavities (ϕ_C). The increasing ϕ_{VO_2} values are referred to as $\phi(P_i)$ ($i = 1$ to 12). In Table 2 the calculated volumic weights (μ_{Id}) are given for specific ideal volume fractions denoted ϕ_i ($i = 0$ to 10).

In Fig. 1, the experimental volumic weights μ_{Obs} are compared to the ideal values μ_{Id}, which are linearly dependent on μ_{POL} and μ_{VO_2}. A pellet made of pure VO_2 ceramic was separately prepared: because of the residual interstices the ϕ_{Obs} value is only 0.91.

II.2. X-Ray Diffraction Analysis

Each composite pellet was analyzed by X-ray diffraction on a D 5000 Siemens diffractometer, using SOCABIM programs, and the changes in multiphase diffraction patterns are observed: in Fig. 2, a typical X-ray diffraction pattern is presented.

—1. The Bragg peaks of vanadium dioxide provide an indication of the distribution of the pigments near both plane faces of the cylindrical pellets (see Appendix).

—2. Two kinds of information are provided by the Bragg peaks of the crystallized LDPE components (see Appendix), dispersed in amorphous host:

[1] To whom correspondence should be addressed.

0022-4596/94 $6.00

TABLE 1
Characteristics of the Pellets

	P1	P2	P3	P4	P5	P6
ϕ_{VO_2}	0.000	0.017	0.040	0.063	0.105	0.130
μ_{Obs} (g cm^{-3})	0.885	0.923	0.949	0.975	1.226	1.245
	P7	P8	P9	P10	P11	P12
ϕ_{VO_2}	0.196	0.270	0.330	0.395	0.550	0.910
μ_{obs} (g cm^{-3})	1.520	1.813	1.948	2.178	2.575	4.273

—the intensities are proportional to the crystalline fraction,

—the broadening of the (110) and (200) reflections are related to the growth of crystallites (orthorhombic cell).

To monitor the preparation process and the final state of the LDPE host, two quantities were systematically measured:

—the $R = (I_{110} + I_{200})/I_T$ ratio is characteristic of the LDPE host (I_{hkl} is the LDPE Bragg peak intensity; I_T is the total intensity due to both amorphous and crystallized components);

—the broadening Δ of the (110) and (200) reflections may be related to the size of crystallites through the classical relation (13)

$$\Delta^2 = (\Delta 2\theta(\text{POL}))^2 - (\Delta 2\theta(VO_2))^2,$$

where

Δ corresponds to the size effect,

$\Delta 2\theta$(POL) is the angular broadening for polymer, and $\Delta 2\theta(VO_2)$ is taken as a standard to obtain the experimental broadening (the (011) peak of monoclinic VO_2 is used).

The (L) sizes are calculated using the classical relation (13)

$$L(hkl) = 0.9\ \lambda/(\Delta \cos \theta),$$

where λ is the Cu$K\alpha$ wavelength (1.54 Å), θ is the Bragg angle of the peak (hkl), and $L(hkl)$ is the mean dimension of the crystallite along the direction parallel to the reciprocal vector (hkl).

TABLE 2
Volume Fractions and Calculated Volume Weights

	$\phi 0$	$\phi 1$	$\phi 2$	$\phi 3$	$\phi 4$	$\phi 5$	$\phi 6$	$\phi 7$	$\phi 8$
ϕ_{VO_2}	0.0	0.1	0.2	0.3	0.4	0.5	0.6	0.7	0.8
μ_{td} (g cm^{-3})	0.915	1.291	1.668	2.044	2.421	2.797	3.174	3.550	3.927

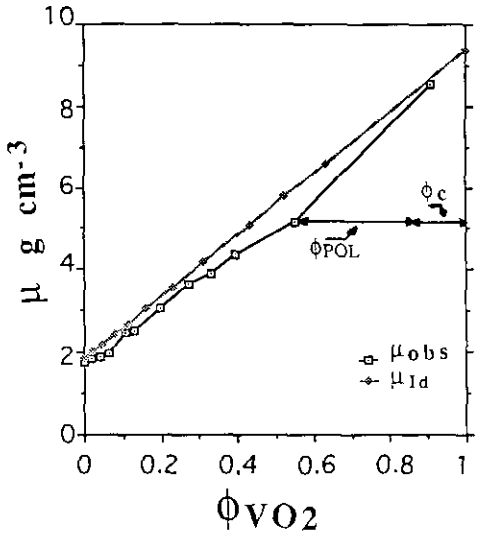

FIG. 1. Experimental and calculated volumic weights (μ_{Id} and μ_{Obs}) for the various composite pellets. ϕ_{POL} is the volume fraction of polymer; ϕ_C is the volume fraction associated with cavities.

The principal results are reported in Table 3. The dimension of the LDPE crystallites slowly increases with increasing volume fraction of VO_2. However, in the (ab) plane of the LDPE crystal, it seems reasonable to assume a nearly constant mean size, with

$$\langle L(hk0) \rangle = 150 \pm 10 \text{ Å}.$$

Such a mean size is a result of the cooling or quenching process and thus can be used to control the preparation procedure. Such control is necessary because of the effect of microstructure on electrical properties; the main feature probably involves the presence of pores and imperfect interfaces in the samples.

II.3. Study of Microstructure

The pellets have been studied by scanning electron microscopy (SEM, JEOL JCM 35 C) linked to an EDS X-

TABLE 3
X-Ray Diffraction Study of Polyethylene Crystal Components[a]

Pi (%)	$(I_1 + I_2)/I_T$	L_1 (Å)	L_2 (Å)
0	0.28	146	110
6.3	0.43	124	112
10.5	0.43	152	128
13	0.37	165	152
19.6	0.66	167	142
27	—	158	—

[a] $L_1 = L(110)$; $L_2 = L(200)$.

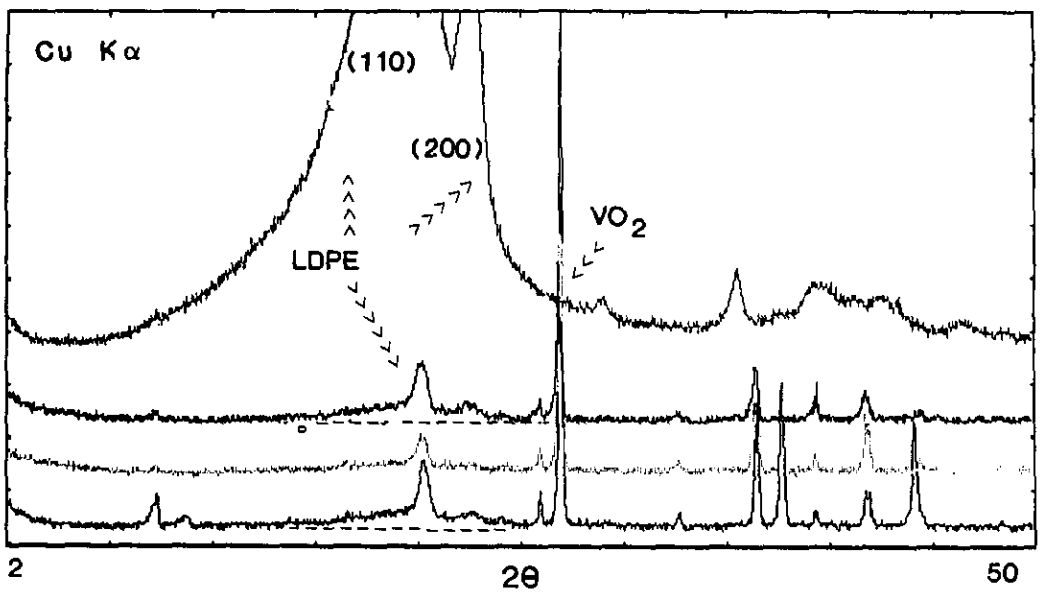

FIG. 2. Typical X-ray diffraction pattern of a composite pellet; the Bragg peaks of VO_2 and polyethylene (LDPE) are visible. The crystallinity of LDPE is determined from the intensity ratio and width of Bragg peaks.

ray microanalysis system (TRACOR TN 524). To investigate the bulk microstructure, we cut cross sections along a diameter of the sample, using a diamond saw. X-ray mapping ($K\alpha$: 4.94 KeV line) correlated to secondary electron micrographs enabled us to identify the VO_2 pigments among the polymer host, at low magnification.

Next, high magnification micrographs have been obtained inside the polymer zone. Typical results are shown in Figs. 3a and 3b, where one can identify the polymer as elongated low-contrast fibers and VO_2 as well-contrasted roughly spherical grains. In Fig. 3a, the size of the VO_2 grains is roughly 5 μm. Furthermore, these grains are linked together to form characteristic twisted chains. In Fig. 3b a fairly dispersed phase can be seen with micrometer- or even submicrometer-sized grains.

Another characteristic feature of the microstructure is shown in Fig. 3c: here the previous chains constitute small bonds between bigger grains in the 30-μm range. This situation is schematized in Fig. 3d and indicates the possibility of electrical continuity through the polymer along the average direction of the bonds. This striking result is analyzed further (Section III) through a percolation model, allowing us to interpret the abnormally low value of the VO_2 ϕ_{lim} volume fraction, above which the high VO_2 conductivity appears in the sample; the transition of VO_2 can then be observed when the temperature increases.

II.4. Electrical Measurements

The electrical measurements are carried out using potentiostat/galvanostat equipment connected to a high-frequency response analyzer. The frequency range is variable from 10^{-1} to 10^6 Hz. The frequency is denoted ω and is expressed in Hz. The pellets are pressed between gold electrodes, first at room temperature, then heated above the transition temperature of VO_2 ($T = 363$ K $> T_c$). Interface effects due to heating were eliminated by thermal cycling.

Each sample is characterized by
—its constant section $S = \pi D^2/4$
—its thickness h (3 to 7 mm)
—its three volume fractions ϕ_{VO_2}, ϕ_{POL}, ϕ_C.

Then, each observed impedance modulus $|Z|$ has to be corrected according to the relation

$$|Z| = z\,(h/S);$$

i.e., $R = \rho\, h/S$ or $C = \varepsilon S/h$, ρ and ε being the resistivity and the dielectric constant.

However, due to imperfect electrode–sample interfaces, only the relative change of $|Z|$ as a function of frequency and volume fraction can yield information about the associated complex impedance function.

In Fig. 4 the experimental complex impedance moduli are shown as a function of ω for P_1 (pure LDPE host), P_6 (intermediate composition), and P_{12} (pure VO_2 pellet), at two temperatures ($T < T_c$ and $T > T_c$). They are represented using logarithmic values:

$$\log|Z| = Y_\phi(\omega) = f_\phi(\log \omega), \quad (\phi \text{ fixed}, \omega \text{ variable}).$$

In the insulating phase ($\phi = 0$), the phase angle is uncertain ($\varphi \sim -\pi/2$); in the metallic (resistive) phase

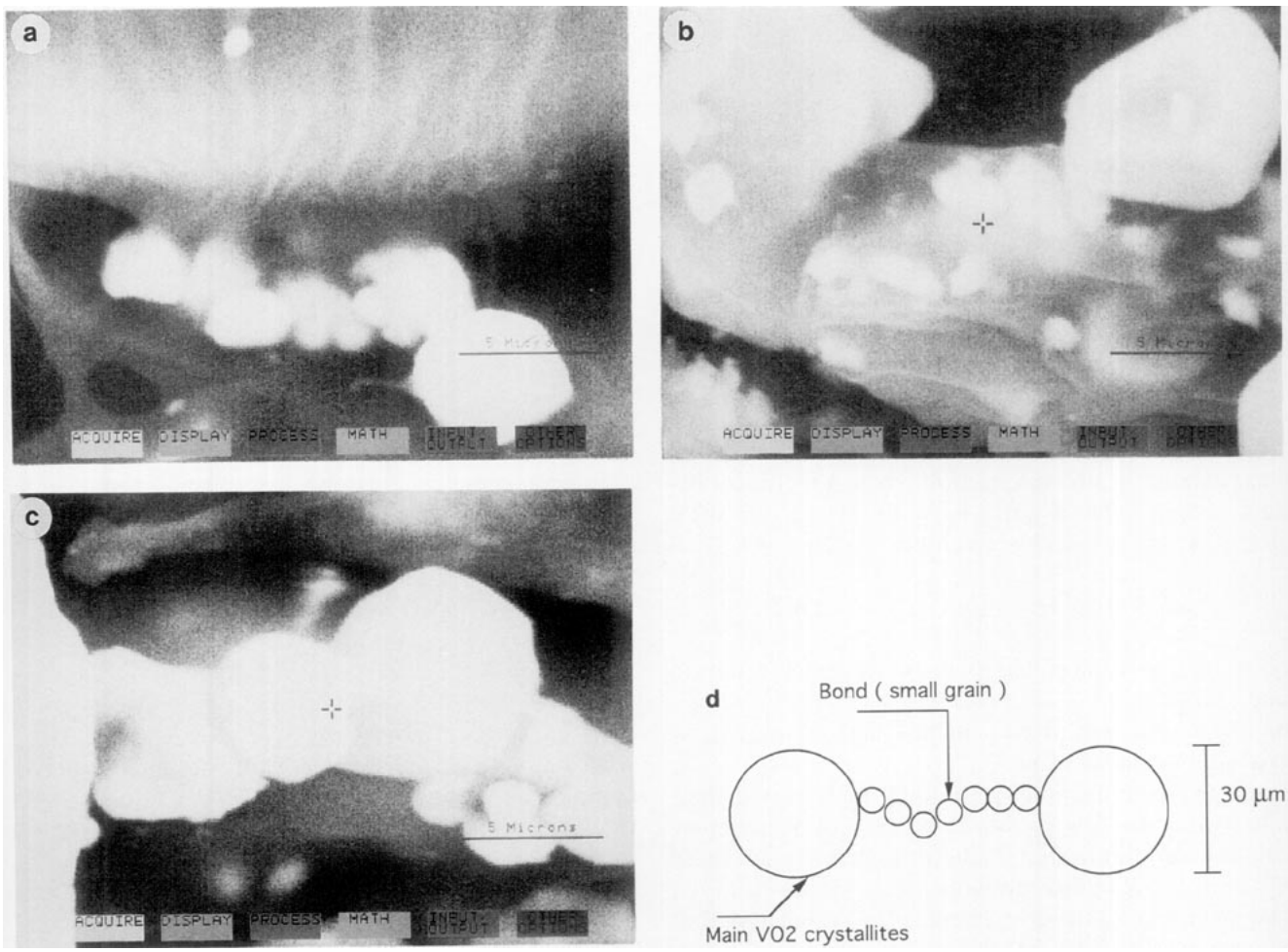

FIG. 3. (a)–(c) Scanning electron microscopy on a composite pellet: VO_2 grains are clearly observed with dimensions ranging from 1 to 40 μm. Between the biggest grains, irregular bridges made of smaller grains are observed. (d) Schematic drawing illustrating such a typical observation.

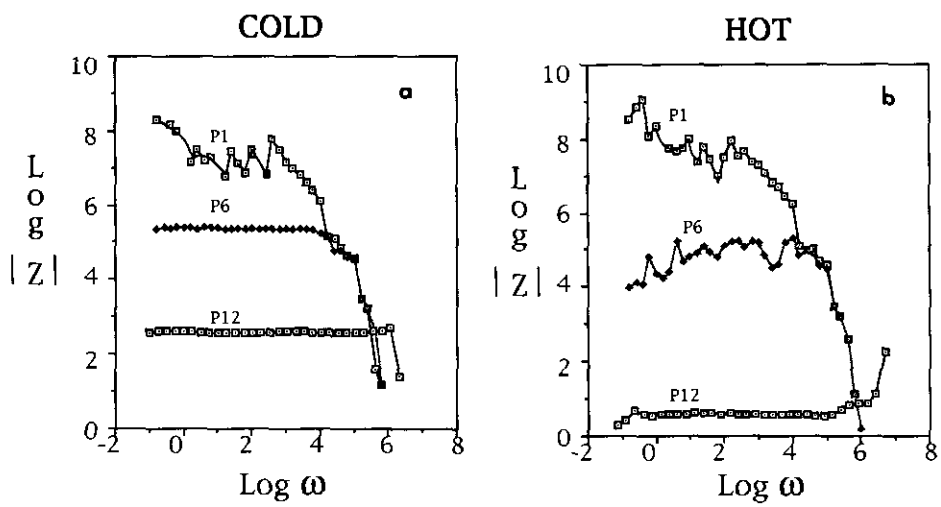

FIG. 4. (a) Experimental complex impedance moduli (logarithmic values) of the samples P1 (pure LDPE host), P6 (intermediate), and P12 (pure VO_2 pellet), as a function of log ω (ω frequency Hz) and at 300 K. (b) Same experiment but at 363 K (90°C) above the transition temperature ($T_c \approx 341$ K).

($\phi = 0.91$; pure VO_2) the phase angle is found to be about $\varphi = 0$.

The change in electrical property is clearly apparent for volume fractions greater than $\phi = 0.20$. Above this approximate concentration, pure resistive behavior of the pellets P_i is observed at room temperature ($T < T_c$): the $\log|Z|$ values are found to be constant in a wide frequency range ($\omega = 10^{-1}$ to ω_{max}).

In Fig. 5 the results are reported using the relation

$$\log|Z| = Y_\omega(\phi) = f_\omega(\phi), \quad (\omega \text{ fixed}, \phi \text{ variable}).$$

The following results are found:

—for low ω values the $\log|Z|$ experimental function, obtained by "smoothing" the distribution of experimental values, exhibits a strong variation when ϕ increases beyond a certain value $\phi_{1/2}$ (for $\omega = 10^3$ Hz, $\phi_{1/2} = 0.25$) such that $Y_\omega(\phi) = \log|Z|$ is given by

$$Y_\omega(\phi_{1/2}) = (Y_\omega(\phi = 0) + Y_\omega(\phi = 1))/2.$$

—for high ω values, $\log|Z|$ does not exhibit such a strong variation.

As a first approach, the $\phi_{1/2}$ values might be defined as "percolation compositions."

The $Y_\omega(\phi)$ experimental functions strongly vary in their profile with ω: for low ω, the (R, C) type of behavior by pellets is clearly indicated while for higher ω values (10^4 to 10^6 Hz), the R regime prevails.

The main feature observed here is the percolative (but progressive) electrical behavior with abnormally low $\phi_{1/2}$ values. In ideal single-sized spheres, various regular packings can be expected for volume fractions such as

$\phi = 0.34$ for diamond type packing
$\phi = 0.68$ for body centered cubic packing
$\phi = 0.74$ for compact packing.

In order to interpret the present results, it was necessary to propose various models using complex impedance calculations.

III. DISCUSSION

To understand the abnormal properties of the experimental functions $Y_\phi(\omega)$ and $Y_\omega(\phi)$, it was necessary to consider various models that represent the composite structures, i.e., the distribution of VO_2 pigments in the polyethylene host.

As a first step, an elementary model (model I) was considered. Single-sized cubic particles were assumed to be regularly distributed, as indicated in Figs. 6a and 6b. The alternate zones of VO_2 pigments and polymer host can be represented as electrical complex impedances (resistance R, capacitance C): see Fig. 6c. From the simple model I and using cubic pigments, it was possible to obtain the linear VO_2 fraction as

$$X = (\phi_{VO_2})^{1/3}.$$

In the case of noncubic symmetry, the model can be easily modified by taking into account shape factors $K_x K_y K_z$ with

$$X_1 = K_x \phi^{1/3}$$

($X_2 = K_y \phi^{1/3}$, $X_3 = K_z \phi^{1/3}$; x, y, z are associated with the three space directions).

Each Z impedance can be described by the relation

$$Z_i = z_i * X/X^2 \quad (\text{i.e., } R = \rho L/L^2).$$

The global impedance $Z(\omega, \phi)$ is a function of ω and ϕ, or X,

$$1/Z(\omega, \phi) = 1/Z_{p_2} + 1/(Z_v + Z_{p_1}),$$

where Z_{p_1} and Z_{p_2} are the impedances of the two polymer components electrically in series (POLY 1) or in parallel (POLY 2), and Z_v is the corresponding one for the VO_2 pigments.

Each Z impedance is assumed to be of an (R, C) type:

$$Z^{-1} = 1/R + jC\omega.$$

Taking into account the various Z components of VO_2 pigments and of POLY 1 (intermediate zones) and POLY 2 polymer parts, the general expression is found to be a function of the linear fraction $X = \phi^{1/3}$:

$$\begin{aligned} Z^{-1} = {} & X^2/(R_V X/((1 + jR_V C_{p_1}\omega) \\ & + R_{p_1}(1 - X)/(1 + jR_{p_1}C_{p_1}\omega)) \\ & + (1 - X^2)/(1 + jR_{p_2}C_{p_2}\omega). \end{aligned}$$

In principle, all the samples might be characterized by only one set of values: R_{p_1}, C_{p_1}, R_{p_2}, C_{p_2}, R_V, C_V. However, each set depends on a preparation process. Thus it can vary with X within some limits.

In model I, the (R, C) values are assumed to be constant, independent of the volume fraction: however, such a model was found to be quite insufficient to explain our experimental results. To improve the initial electrical characterization, it was necessary to take into account the percolation effects via adjusted composition-dependent impedance functions. Such critical behaviors in composites were previously described by Coniglio *et al.* (14) and Bergman and co-workers (15).

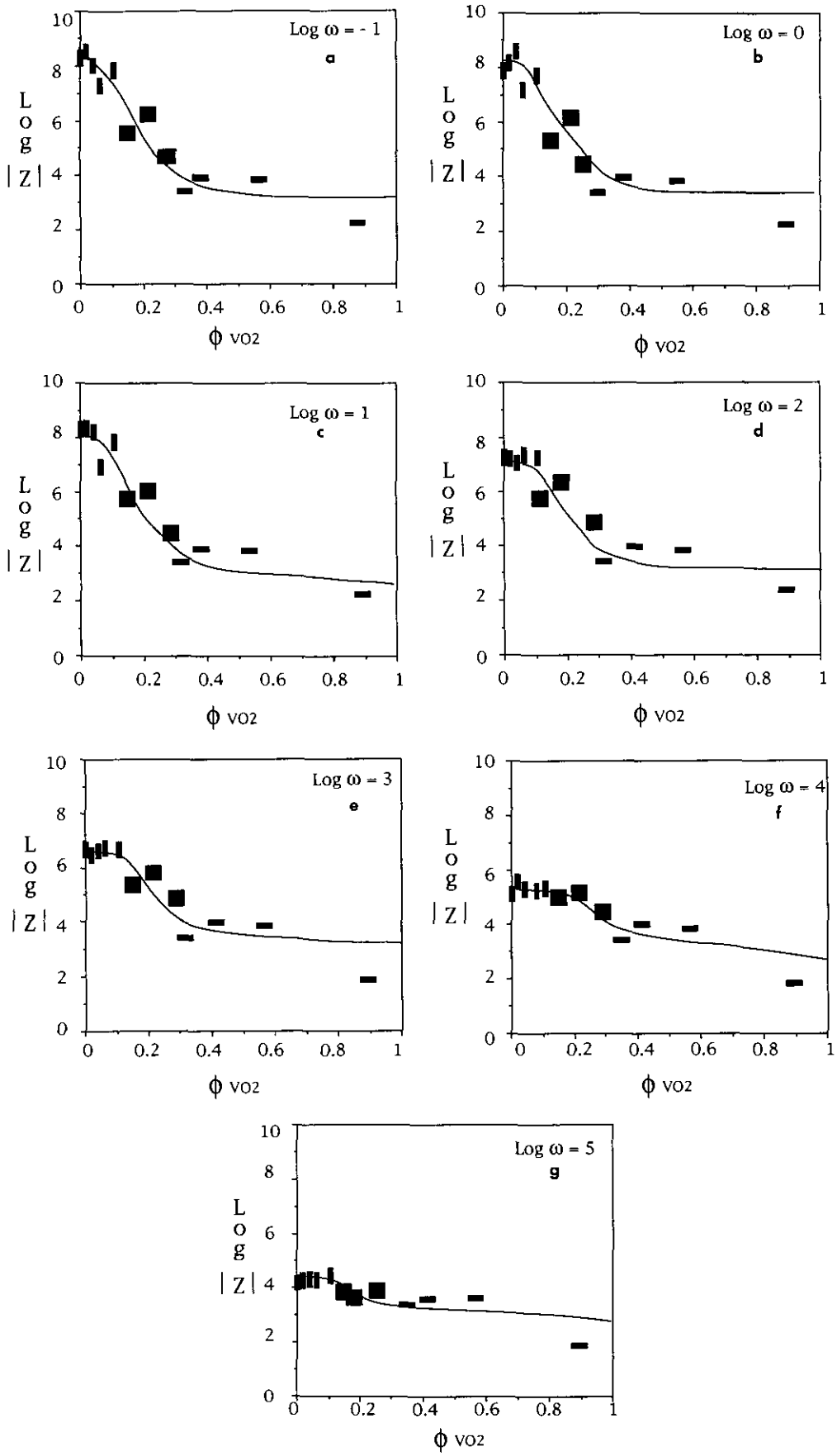

FIG. 5. Experimental log $|Z|$ values as a function of volume fraction ϕ_{VO_2} for the samples P_i (i = 1 to 12) and at a fixed ω_i frequency. (a) $\omega_1 = 10^{-1}$, (b) $\omega_2 = 1$, (c) $\omega_3 = 10$, (d) $\omega_4 = 10^2$, (e) $\omega_5 = 10^3$, (f) $\omega_6 = 10^4$, (g) $\omega_7 = 10^5$.

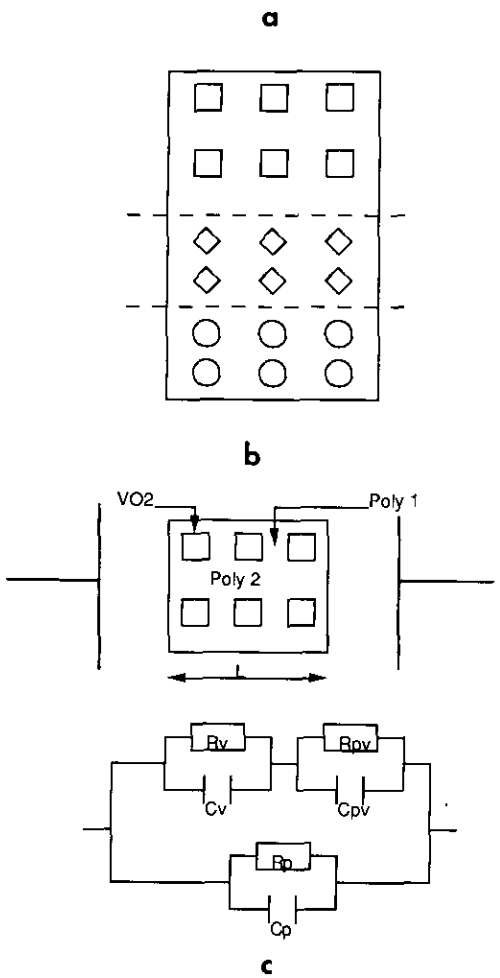

FIG. 6. Schematic representation of the composite pellets. Electrodes are represented to justify the present (R, C) model. (a) The symbols (□, ◇, ○) represent different pigments. (b) Definition of the various domains: POLY 1 is for polyethylene affected by VO_2 pigments. POLY 2 is for polyethylene with properties independent of VO_2. (c) Electrical model: (R_v, C_v) are for VO_2 pigments. (R_{pv}, C_{pv}) are for POLY 1 (in series). (R_p, C_p) are for POLY 2 (in parallel).

To take into account percolation effects, model II was adapted with the following features:

—1. In some regions between VO_2 pigments, a percolation distance between grains is assumed to exist: the associated percolation composition is denoted by ϕ_{lim} and taken as equal to 0.30. In the case of single-sized spherical grains the ϕ_{lim} value should be directly related to the classical compactness of sphere assemblies.

—2. Due to the presence of variable grain sizes dispersed through the LDPE host, the (R, C) values of polymer between VO_2 grains (POLY 1) are assumed to be a function of the volume fraction ϕ_{VO_2}. As the fraction ϕ increases the ceramic behavior becomes more prominent. An empirical function is postulated.

For $0 < \phi < \phi_{lim}$, the variation is described by

$$Z_{p_m} = Z_p \exp - A\phi^n \quad (n > 1);$$

i.e., for $\phi = 0$, $Z_{p_m} = Z_p$.

For $\phi > \phi_{lim}$, the variation is taken to be

$$Z_{p_m} = Z_{p_m}(\phi_{lim}) \exp(-B(\phi - \phi_{lim})),$$

with $Z_{p_m} = Z_m$ for $\phi = 1$.

The A and B parameters are constants calculated for $\phi = \phi_{lim}$ and $\phi = 1$ as boundary conditions: they express the increasing percolation effect due to the distribution of grains. Among the various values of n tested to obtain a unique good fit for all the experimental results, $n = 2$ was chosen: this corresponds to Gaussian-like behavior. The second function was chosen to express two effects: while the biggest grains are assumed to be subject to compact packing, the population of the smallest grains can occupy the residual interstices and provide a contribution to the electrical properties.

In Fig. 7, the functions resulting of Model II are represented. Figure 7a shows the variation of Z_{p_m} as a function of the volume fraction ϕ and for fixed ω values. Figures 7b and 7c respectively represent (i) the values of log (Z) calculated for fixed volume fractions as a function of log ω, and (ii) the values of log (Z) calculated for fixed ω frequencies (denoted 1 to 7) as a function of the volume fraction ϕ.

The various functions represented on the figures were obtained using only one set of (R, C) values to obtain a qualitative agreement with the experimental results at 25°C:

$$R_m = R_V = 10^4\ \Omega \qquad C_m = C_V = 10^{-12}\ \text{F}$$
$$R_p = 10^9\ \Omega \qquad C_p = 10^{-10}\ \text{F}$$
$$\phi_{lim} = 0.30.$$

At 353 K (80°C; i.e., $T > T_c$) the electrical resistance of VO_2 pigments is assumed to be that observed in pure VO_2 pellets. In Fig. 8 a simulation of the transition is presented for the frequency $\omega_4 = 10^2$ Hz: the electrical transition is clearly observable for $\phi > 0.25$.

Under this assumption, it is possible to simulate the $\log Z = f_\omega(\phi)$ functions, leading to acceptable agreement with the present experimental data. Obviously, model II could be improved by adjusting the individual R and C values of each sample. In fact the main result of this modeling is the determination of a percolation composition denoted ϕ_{lim} in model II. Experimentally, the $\phi_{1/2}$ values vary with frequency from about 0.25 to 0.33, so these values cannot directly yield the percolation composition. However, they are not far from the adjusted uniquely modeled ϕ_{lim} value.

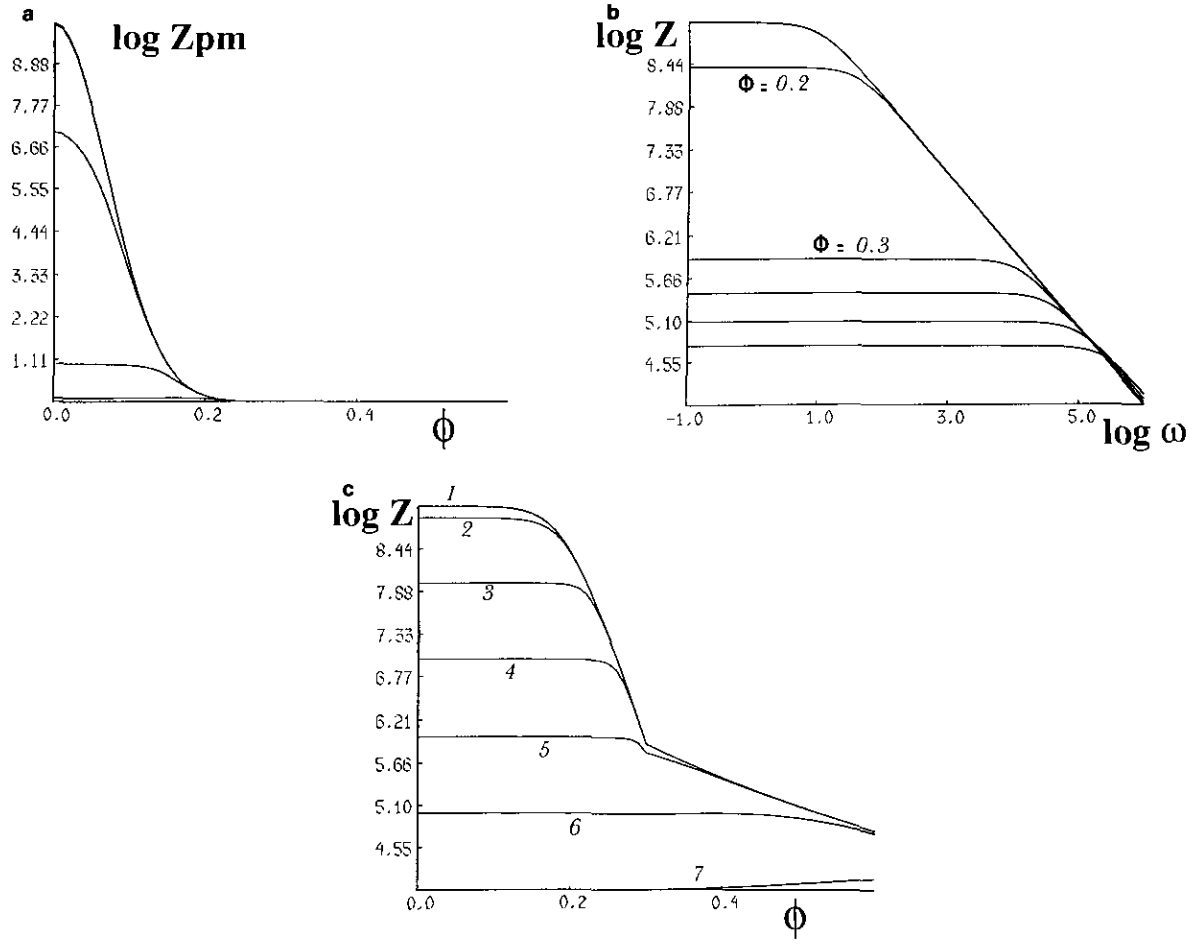

FIG. 7. Complex impedance modulii in the case of percolation. (a) Variation of the logarithm of Zpm (impedance modulus of the POLY 1 component) according to model II: log(Zpm) is affected by the presence of VO_2 pigments (it varies with ϕ for fixed ω values). The function is calculated using a percolation limit with $\phi_{lim} = 0.30$. The ω_i values lead to log(Zpm) curves that increase from 10^{-1} to 10^{+5} Hz (see text); i.e., for $\phi = 0$, this Zpm impedance modulus decreases with ω. (b) Calculated log|Z| curves as a function of log ω, using the percolation hypothesis (model II): for fixed ϕ values the various calculated log|Z| functions are quite different and exhibit resistive–capacitive characteristic changes when log ω varies. Two volume fractions 0.2 and 0.3 are indicated. (c) Calculated log|Z| curves as a function of volume fraction ϕ in the case of model II: the percolation is well simulated with $\phi_{1/2}$ varying from 0.25 to about 0.33; such a result is obtained using the adjusted $\phi_{lim} = 0.30$ value. The fixed ω_i are denoted from 1 to 7 (10^{-1} to 10^{+5} Hz as indicated in Fig. 5).

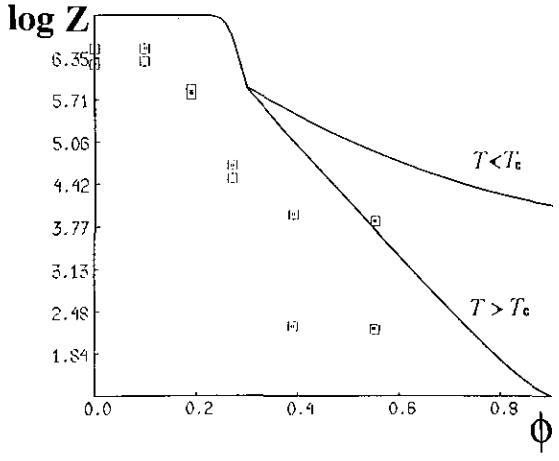

FIG. 8. Simulation of the transition: the log(Z) calculated functions are represented as a function of ϕ, using the percolation hypothesis of model II for two temperatures ($T < T_c$ and $T > T_c$) and at a fixed $\omega = 10^2$ Hz (ω_4) value. The transition is observable for $\phi > 0.20$. Some experimental points are reported (empty squares).

IV. CONCLUSION

In this study it was clearly shown that composite materials, prepared from mixed polymer and ceramic pigments, can be characterized by percolative electrical properties. A critical composition $\phi_{1/2}$ can be defined, which varies with frequency. At $\omega = 10^2$ or 10^3 Hz the $\phi_{1/2}$ value is about 0.25.

The insulator–metal transition of VO_2 can be observed in impedance measurements when the volume fraction is greater than $\phi_{1/2}$.

Such a result can be explained in terms of progressive electrical contacts due to the presence of a wide variety of grain sizes irregularly distributed in the polymer host. A percolation model allowed us to interpret all the experimental Z values: a unique ϕ_{lim} parameter (close to the variable $\phi_{1/2}$ values) was introduced in the model to simulate all the impedance functions.

SEM observations seem to confirm such a description of percolation in these composite materials.

APPENDIX

The crystallographic data for LDPE and the VO_2 ceramic are as follows:

—1. for LDPE the space group is $P2_1/n2_1/a2_1/m$ and the cell parameters are $a = 7.40$ Å, $b = 4.93$ Å, $c = 2.53$ Å; the melting point is about 120°C;

—2. for the insulating phase of VO_2 the space group is $P2_1/c$ and the cell parameters (10) at 298 K are $a = 5.754$ Å, $b = 4.525$ Å, $c = 5.386$ Å, $\beta = 122.60°$; the transition temperature is $T_c = 341$ K (68°C) for pure VO_2; the conductivity is characterized close to T_c by a ratio $\sigma(up)/\sigma(low) = 10^3$ in polycrystals.

—3. for the VO_2 metallic phase (10) the structure is that of tetragonal rutile with $a = 4.556$ Å, $c = 2.851$ Å.

ACKNOWLEDGMENT

We gratefully acknowledge our colleagues Professor Sebaoun and Dr. E. Lanza for the use of their electrical equipment.

REFERENCES

1. J. B. Goodenough, *J. Solid State Chem.* **3,** 490 (1971).
2. G. Villeneuve, A. Bordet, A. Casalot et P. Hagenmuller, *Mater. Res. Bull.* **6** (1971).
3. P. Lederer, H. Launois, J. P. Pouget, A. Casalot, and G. Villeneuve, *J. Phys. Chem. Solids* **33,** 1969 (1972).
4. J. B. Goodenough, "Les oxydes des métaux de transition," 1ère Ed. Gauthier–Villars, Paris 1973.
5. A. Akroune, Thèse. Université de Provence, 1984.
6. A. Akroune, J. Claverie, A. Tazairt, G. Villeneuve et A. Casalot, *Phys. Status Solidi A* **89** (1985).
7. J. C. Rakotoniaina, R. Tamellin, J. R. Gavarri, G. Vacquier, and W. Chodckiewicz, in "Proceed.: Comm. Coll. Int. Reg. Eur. Céramiques, Lyon," 1991.
8. J. C. Rakotoniaina, R. Tamellin, J. R. Gavarri, G. Vacquier, W. Chodckiewicz, et C. Cesari, in "Com. Gen. Conf. of Cond. Mat. Div. Prague," 1992.
9. J. R. Gavarri, in "Com. 5ème Journée de la Chimie (SFC-PACA) Nice–Sophia–Antipolis, 1992.
10. J. C. Rakotoniaina, R. Mokrani-Tamellin, J. R. Gavarri, G. Vacquier, A. Casalot, and G. Calvarin, *J. Solid State Chem.* **103,** 81 (1993).
11. J. C. Lee, G. V. Jorgenson, and R. J. Lin, *Proc. SPIE—Int. Soc. Opt. Eng.* **692,** 2 (1986).
12. S. M. Babulanam, T. S. Erikson, G. A. Niklasson, and C. G. Granquist, *Proc. SPIE—Int. Soc. Opt. Eng.* **692,** 8 (1986).
13. A. Guinier. "Théorie et techniques de la radiocristallographie," p. 359. Dunod, Paris, 1964.
14. A. Coniglio, M. Daoud, and H. J. Herrmann, *J. Phys. A* **22,** 4189 (1989).
15. D. J. Bergman, *Physica A,* **157,** 72 (1989); H. Rosenthal and D. J. Bergman, *J. Phys. A* **22,** 3629 (1989).